

Photonic Generation of a Phase-Coded Microwave Waveform With Ultrawide Frequency Tunable Range

Liang Gao, *Student Member, IEEE*, Xiangfei Chen, *Senior Member, IEEE*, and Jianping Yao, *Fellow, IEEE*

Abstract—Photonic generation of a phase-coded microwave waveform with ultrawide frequency tunable range using two polarization modulators (PolMs) is proposed and experimentally demonstrated. The first PolM (PolM1) is used to control the polarization direction of a linearly polarized light wave to have an angle of 45° or 135° relative to one principal axis of the second PolM (PolM2). PolM2 operates in conjunction with a polarization controller and a polarizer as an equivalent Mach–Zehnder modulator (MZM). Depending on the polarization direction of the incident light wave, the equivalent MZM is biased at the opposite slopes of the transfer function. Thus, by applying a binary coding signal with a switching voltage of V_π to PolM1, a π phase-coded microwave waveform is generated. The key significance of the technique is that a phase-coded microwave waveform with an ultrawide frequency tunable range can be generated. The technique is experimentally evaluated. The generation of a frequency-tunable phase-coded microwave waveform with a frequency at 10, 20, 30, and 40 GHz is demonstrated.

Index Terms—Microwave photonics, microwave signal generation, phase coding, radar pulse compression.

I. INTRODUCTION

MICROWAVE pulse compression has been widely employed in modern radar systems to increase the range resolution [1]. Microwave pulse compression can be achieved based on matched filtering using a chirped or phase-coded microwave pulse. However, the bandwidth and frequency of an electronically generated microwave pulse are usually low, restricted by the speed of digital electronics. Therefore, the photonic generation of frequency-chirped or phase-coded microwave signals has been a topic of interest thanks to the large bandwidth and high frequency offered by modern photonics [2]–[12]. Numerous techniques have

Manuscript received January 27, 2013; revised March 3, 2013; accepted March 14, 2013. Date of publication March 20, 2013; date of current version April 25, 2013. This work was supported in part by the Natural Science and Engineering Research Council of Canada. The work of L. Gao was supported in part by a Scholarship from the China Scholarship Council.

L. Gao is with the Microwave Photonics Research Laboratory, School of Electrical Engineering and Computer Science, University of Ottawa, ON K1N 6N5, Canada, and also with the National Laboratory of Solid State Microstructures and College of Engineering and Applied Sciences, Nanjing University, Nanjing 210093, China.

X. Chen is with the National Laboratory of Solid State Microstructures and College of Engineering and Applied Sciences, Nanjing University, Nanjing 210093, China.

J. Yao is with the Microwave Photonics Research Laboratory, School of Electrical Engineering and Computer Science, University of Ottawa, ON K1N 6N5, Canada (e-mail: jpyao@eecs.uottawa.ca).

Color versions of one or more of the figures in this letter are available online at <http://ieeexplore.ieee.org>.

Digital Object Identifier 10.1109/LPT.2013.2253455

been proposed to generate a phase-coded microwave waveform [7]–[12]. A phase-coded microwave pulse can be generated by optical pulse shaping using a spatial light modulator (SLM) [7]. The key advantage of an SLM-based system is its flexibility since an SLM can be updated in real time. The major limitation is the complexity due to the fiber-to-space and space-to-fiber coupling. All-fiber based systems have also been proposed. For example, a phase-coded microwave waveform can be generated using an all-fiber Mach–Zehnder interferometer or a Sagnac interferometer incorporating a phase modulator [8], [9]. The phase coding is performed by applying a binary phase-coding signal to the phase modulator. The major limitation of the systems is the poor stability because of the use of an interferometer, which is sensitive to environmental variations. In [10], an approach with stable operation employing a polarization modulator (PolM) was proposed. Due to the use of a length of polarization-maintaining fiber (PMF) to generate two orthogonally polarized optical light waves, the frequency is not tunable. The problem was solved in [11], where a polarization-maintaining fiber Bragg grating (PM-FBG) was used to generate two orthogonally polarized optical sidebands with tunable wavelength spacing. Recently, we proposed a phase coding system with precisely π phase shift using a PM-FBG to select the optical carrier and one of the sidebands of a phase-modulated signal [12]. Since the phase difference between the two sidebands of a phase-modulated signal is inherently π , a phase-coded microwave waveform with precise π phase shift was generated. Again, the frequency tunable range is small due to the limited bandwidth of the PM-FBG.

In this letter, we propose and experimentally demonstrate a photonic technique to generate a phase-coded microwave waveform with an ultrawide frequency tunable range. The system consists mainly of two PolMs without using any optical filters. In the system, a linearly polarized light wave from a laser diode (LD) is sent to the first PolM (PolM1), with the polarization direction of the light wave oriented with an angle of 45° relative to one principal axis of PolM1, to which a phase coding signal with a switching voltage of the half-wave voltage is applied. Thus, the polarization direction of the linearly polarized light wave will be controlled to have an angle of 45° or 135° relative to one principal axis of the second PolM (PolM2). PolM2 operates in conjunction with a polarization controller (PC) and a polarizer as a Mach–Zehnder modulator (MZM). Depending on the polarization state of the incident light wave, the MZM is biased at the opposite slopes of the transfer function. Thus, a π phase-coded microwave waveform

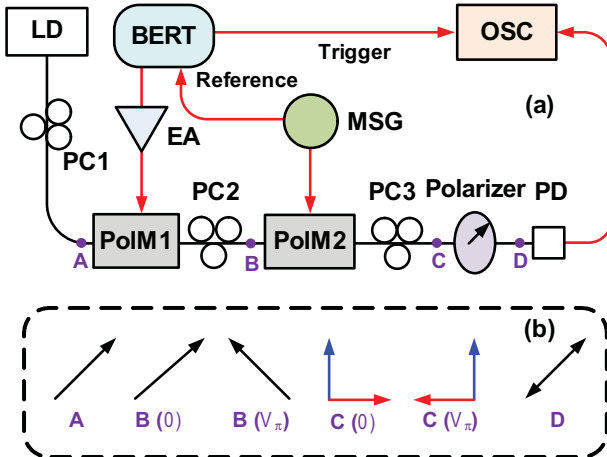


Fig. 1. (a) Schematic of the proposed phase-coded microwave waveform generation system. (b) Polarization direction of the light wave at different locations. LD: laser diode. PC: polarization controller. PolM: polarization modulator. BERT: bit error rate tester. EA: electrical amplifier. MSG: microwave signal generator. PD: photodetector. OSC: oscilloscope.

is generated. Since no frequency or wavelength dependent components are employed, the system has an ultrawide frequency tunable range, with the highest frequency only limited only by the bandwidths of the PolMs and the photodetector (PD). The proposed technique is experimentally evaluated. The generation of a frequency tunable phase-coded microwave waveform with a tunable frequency at 10, 20, 30, and 40 GHz is demonstrated.

II. PRINCIPLE

The schematic diagram of the proposed phase-coded microwave waveform generation system is shown in Fig. 1. A light wave generated by a LD is sent to PolM1 via a polarization controller (PC1). The polarization direction of the light wave is adjusted to have an angle of 45° relative to one principal axis of PolM1. PolM2 is connected to PolM1 via PC2 to align the principal axes of PolM2 with those of PolM1. PolM2 is operating with PC3 and the polarizer as a MZM with its bias point at the opposite slopes of the transfer function depending on the polarization direction of the incident light wave to PolM2. Note that to ensure that the equivalent MZM is biased at the quadratic point, PC3 is used to introduce a static phase difference of $\pi/2$ between the two polarization directions. A π phase-coded optical signal is obtained at the output of the polarizer, which is then converted to a microwave waveform at the PD.

A PolM is a special phase modulator that supports both the transverse-electric (TE) and transverse-magnetic (TM) modes with opposite phase modulation indices [13]. When the voltage applied to PolM1 is 0, the electrical fields of the output optical signal from PC3 along the two orthogonal directions are given by

$$\begin{bmatrix} E_x \\ E_y \end{bmatrix} = \frac{\sqrt{2}}{2} E e^{j\omega_0 t} \begin{bmatrix} e^{j\pi/2} [J_0 + j J_1 e^{j\omega_m t} - j J_1 e^{-j\omega_m t}] \\ J_0 - j J_1 e^{j\omega_m t} + j J_1 e^{-j\omega_m t} \end{bmatrix} \quad (1)$$

where E is the amplitude of the electrical field of the optical carrier, J_n is the n^{th} -order Bessel function of the first kind, and ω_0 and ω_m are the angular frequencies of the optical

carrier and the microwave signal, respectively. A static phase difference of $\pi/2$ between E_x and E_y is introduced by PC3. Note that under small-signal modulation condition, only the optical carrier and the $\pm 1^{\text{st}}$ sidebands are considered in (1).

The signal at the output of the PD is given by

$$\begin{aligned} i_1 &= R \left| \frac{\sqrt{2}}{2} E_x + \frac{\sqrt{2}}{2} E_y \right|^2 \\ &= \frac{1}{2} E^2 R \left[J_0^2 + 4 J_1^2 \sin^2(\omega_m t) - 4 J_0 J_1 \sin(\omega_m t) \right] \end{aligned} \quad (2)$$

where R is the responsivity of the PD. The microwave current at the output of the PD is expressed as

$$i_{RF1} = -2 E^2 R J_0 J_1 \sin(\omega_m t) \quad (3)$$

When the voltage applied to PolM1 is V_π , which is the half-wave voltage, the polarization direction of the incident light wave to PolM2 will be rotated by 90° from 45° to 135° [12], [14]. The electrical fields of the output optical signal from PC3 along the two orthogonal directions are given by

$$\begin{bmatrix} E_x \\ E_y \end{bmatrix} = \frac{\sqrt{2}}{2} e^{j\omega_0 t} \begin{bmatrix} e^{j3\pi/2} [J_0 + j J_1 e^{j\omega_m t} - j J_1 e^{-j\omega_m t}] \\ J_0 - j J_1 e^{j\omega_m t} + j J_1 e^{-j\omega_m t} \end{bmatrix} \quad (4)$$

The signal at the output of the PD is given by

$$\begin{aligned} i_2 &= R \left| \frac{\sqrt{2}}{2} E_x + \frac{\sqrt{2}}{2} E_y \right|^2 \\ &= \frac{1}{2} E^2 R \left[J_0^2 + 4 J_1^2 \sin^2(\omega_m t) + 4 J_0 J_1 \sin(\omega_m t) \right] \end{aligned} \quad (5)$$

The microwave current at the output of the PD is

$$\begin{aligned} i_{RF2} &= 2 E^2 R J_0 J_1 \sin(\omega_m t) \\ &= -2 E^2 R J_0 J_1 \sin(\omega_m t + \pi) \end{aligned} \quad (6)$$

As can be seen, there is a π phase shift between the microwave signal in (3) and (6). Note that under small-signal modulation condition, the second-order harmonic is small and ignored in (3) and (6).

III. EXPERIMENT AND RESULTS

An experiment based on the configuration shown in Fig. 1 is carried out. A light wave at 1550 nm from the LD (Agilent N7714A) is sent to PolM1 via PC1. PolM2 is connected to PolM1 via PC2. The PolMs (Versawave) have a 3-dB bandwidth of 40 GHz and a half-wave voltage of 3.5 V. Then, the light wave is sent to a polarizer through PC3. The optical signal from the polarizer is sent to a PD (U²T 50 GHz) for optical-to-electrical conversion. The electrical signal from the PD is monitored by an oscilloscope (OSC, Agilent DCA-J 86100C). A binary phase-coding signal is generated by a bit error-rate tester (BERT, Agilent N4901B), and it is applied to PolM1 after amplified by an electrical amplifier (EA, Multilink MTC5515-2). A sinusoidal microwave signal tunable from 0.25 MHz to 40 GHz is applied to PolM2 as a microwave carrier, generated by a microwave signal generator (MSG, Agilent E8254A).

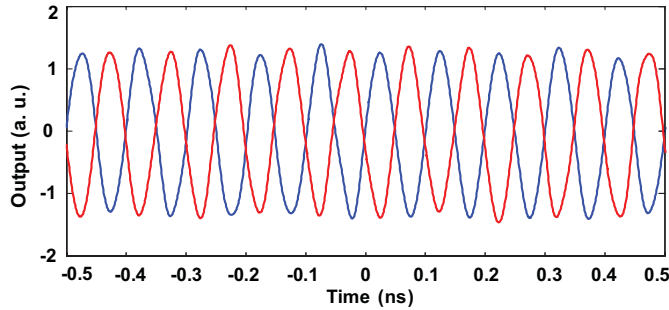


Fig. 2. Microwave waveforms of a 10-GHz microwave signal when the switching voltage is 0 V (blue line), and the switching voltage is the half-wave voltage of the PolM (red line).

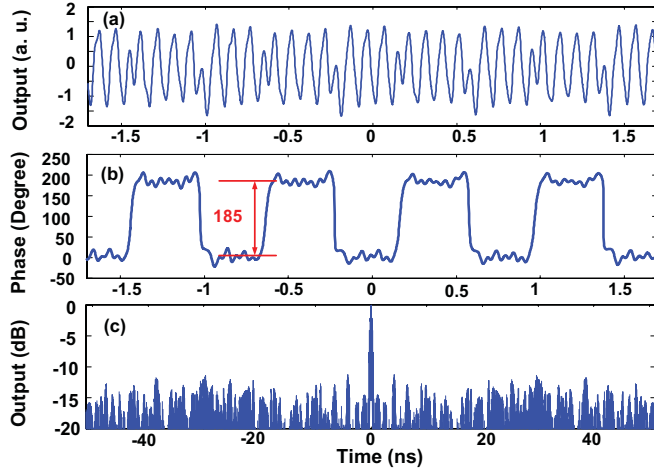


Fig. 3. (a) Generated 10-GHz phase-coded microwave waveform. (b) Recovered phase information from the phase-coded microwave waveform in (a). (c) Calculated autocorrelation of the phase-coded microwave waveform with a carrier frequency at 10 GHz, and a PRBS phase-coding signal with a length of 128 bit at 2.5 Gb/s.

We first study the complementary operation of the equivalent MZM when the polarization direction of the incident light wave is switched from 45° to 135° by changing a switching voltage from 0 to V_π , applied to PolM1 via the DC port, where V_π is 17.5 V for a DC input. A microwave waveform at 10 GHz at the output of the PD is shown in Fig. 2 (blue line), corresponding to the switching voltage to PolM1 is 0 V. Then, when the switching voltage is increased to the half-wave voltage, a complementary microwave signal is obtained, which is also shown in Fig. 2 (red line). As can be seen, a π phase shift is achieved by switching the voltage from 0 to V_π .

To demonstrate the phase-coding capability, a 10-GHz phase-coded microwave waveform is first generated. The phase-coding signal is a “0101” digital sequence of 2.5 Gb/s. Fig. 3(a) shows the waveform of the phase-coded microwave waveform and Fig. 3(b) shows the phase information recovered from the phase-coded waveform using the Hilbert transform. As can be seen, the phase shift is 185° , which is close to the theoretical value of 180° . The phase shift error is mainly caused by the small deviations of the switching voltage applied to PolM1. Then, a pseudo-random bit sequence (PRBS) phase-coding signal at 2.5 Gb/s with a length of 128 bits is applied to PolM1, the corresponding phase-coded microwave signal is generated. To show the pulse compression capability,

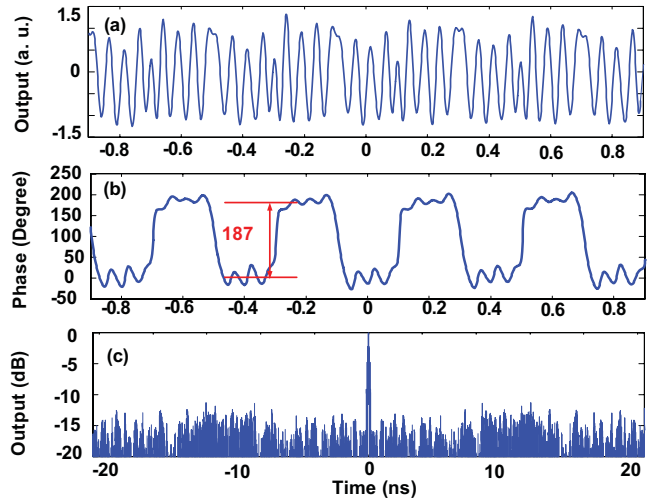


Fig. 4. (a) Generated 20-GHz phase-coded microwave waveform. (b) Recovered phase information from the phase-coded microwave waveform in (a). (c) Calculated autocorrelation of the phase-coded microwave waveform with a carrier frequency of 20 GHz, and a PRBS phase-coding signal with a length of 128 bit at 5 Gb/s.

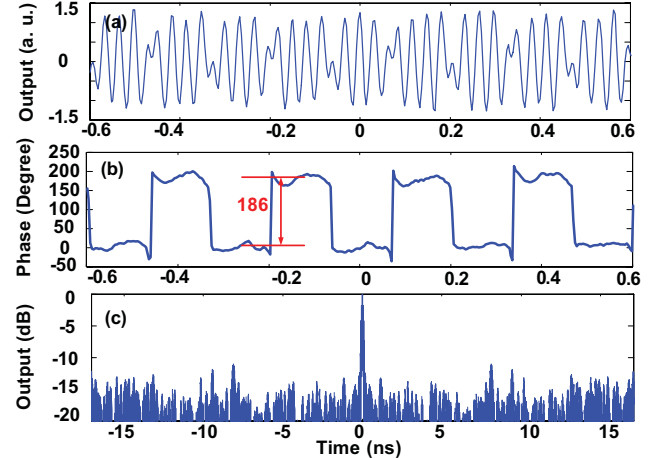


Fig. 5. (a) Generated 30-GHz phase-coded microwave waveform. (b) Recovered phase information from the phase-coded microwave waveform in (a). (c) Calculated autocorrelation of the phase-coded microwave waveform with a carrier frequency of 30 GHz, and a PRBS phase-coding signal with a length of 128 bit at 7.5 Gb/s.

an autocorrelation is calculated and the result is shown in Fig. 3(c). The autocorrelation peak has a 3-dB width of a 0.43 ns, corresponding to a pulse compression ratio (PCR) of about 119.1. The PCR is defined as the ratio of the temporal width of the transmitted pulse to that of the compressed pulse. The peak-to-sidelobe ratio (PSR) is defined as the ratio of the power of the mainlobe to that of the sidelobe. In the experiment, the PSR is calculated to be about 11.3 dB, which is very high due to an accurate π phase shift.

To evaluate the frequency tunability of the proposed system, the frequency of the phase-coded microwave waveform is tuned at three other frequencies of 20, 30 and 40 GHz. Fig. 4(a) shows the waveform of the phase-coded microwave waveform at 20 GHz. Again, the phase-coding signal is a “0101” digital sequence, but with a higher bit rate of 5 Gb/s. The recovered phase information is given in Fig. 4(b). Then,

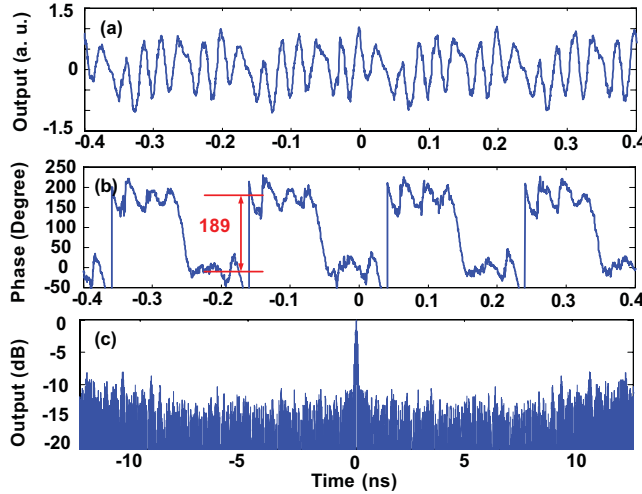


Fig. 6. (a) Generated 40-GHz phase-coded microwave waveform. (b) Recovered phase information from the phase-coded microwave waveform in (a). (c) Calculated autocorrelation of the phase-coded microwave waveform with a carrier frequency of 40 GHz, and a PRBS phase-coding signal with a length of 128 bit at 10 Gb/s.

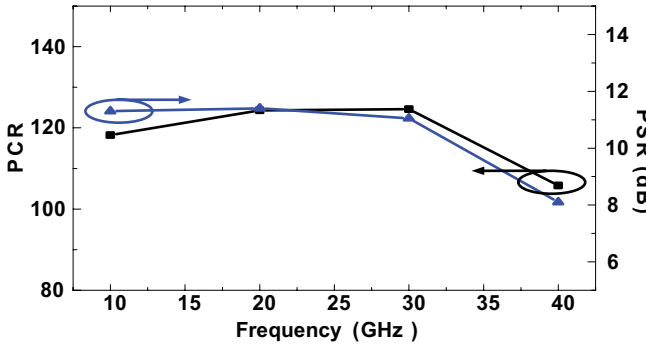


Fig. 7. PCR and PSR when the frequency of the generated phase-coded microwave waveform is tuned at 10, 20, 30, and 40 GHz.

a PRBS phase-coding signal at 5 Gb/s with a length of 128 bits is applied to PolM1. An autocorrelation is calculated and the result is shown in Fig. 4(c). Again, a highly compressed pulse is observed.

Fig. 5(a) shows the waveform of the phase-coded microwave waveform at 30 GHz. The phase-coding signal is a “0101” digital sequence with a data rate at 7.5 Gb/s. Then, a PRBS phase-coding signal at 7.5 Gb/s with a length of 128 bits is applied to PolM1. An autocorrelation is calculated and the result is shown in Fig. 5(c). As can be seen, the pulse is highly compressed.

Fig. 6(a) shows the waveform of the phase-coded microwave waveform at 40 GHz. The phase-coding signal is a “0101” digital sequence at 10 Gb/s. Then, a PRBS phase-coding signal at 10 Gb/s with a length of 128 bits is applied to PolM1. An autocorrelation is calculated and the result is shown in Fig. 5(c). Again, the pulse is highly compressed.

The PCRs and PSRs at different frequencies are shown in Fig. 7. The PCRs are identical to those reported in [12] due to an accurate π phase shift in both techniques, and they are in accordance with the theoretical value of 128. The PSRs are larger than those in [11] and [12], because of the use of

an optical filter in [11] and [12], which would introduce a loss, leading to a reduced signal-to-noise ratio (SNR) of the generated waveform. Note that, the relatively lower PCR and smaller PSR at 40 GHz are caused by the poorer SNR resulted from the higher loss of PolM2 at a higher frequency.

IV. CONCLUSION

A novel and simple photonic approach to generating a phase-coded microwave waveform with an ultrawide frequency tunable range was proposed and demonstrated. The key of the technique is the use of the equivalent MZM which functions in a complementary manner when the polarization direction of the incident light wave is switched between 45° and 135° . A π phase-shifted microwave waveform was generated by switching the bias point, which was done by using another PolM driven by a binary phase-coding signal. Due to the inherent complementary nature of the operation of the equivalent MZM, a precise π phase shift was resulted.

REFERENCES

- [1] M. Skolnik, “Role of radar in microwaves,” *IEEE Trans. Microw. Theory Tech.*, vol. 50, no. 3, pp. 625–632, Mar. 2002.
- [2] J. Chou, Y. Han, and B. Jalali, “Adaptive RF-photonic arbitrary waveform generator,” *IEEE Photon. Technol. Lett.*, vol. 15, no. 4, pp. 581–583, Apr. 2003.
- [3] M. H. Khan, *et al.*, “Ultrabroad-bandwidth arbitrary radiofrequency waveform generation with a silicon photonic chip-based spectral shaper,” *Nature Photon.*, vol. 4, pp. 117–122, Feb. 2010.
- [4] P. Ghelfi, F. Scotti, F. Laghezza, and A. Bogoni, “Photonic generation of phase-modulated RF signals for pulse compression techniques in coherent radars,” *J. Lightw. Technol.*, vol. 30, no. 11, pp. 1638–1644, Jun. 1, 2012.
- [5] A. Zeitouny, S. Stepanov, O. Levinson, and M. Horowitz, “Optical generation of linearly chirped microwave pulses using fiber Bragg gratings,” *IEEE Photon. Technol. Lett.*, vol. 17, no. 3, pp. 660–662, Mar. 2005.
- [6] C. Wang and J. P. Yao, “Chirped microwave pulse compression using a photonic microwave filter with a nonlinear phase response,” *IEEE Trans. Microw. Theory Tech.*, vol. 57, no. 2, pp. 496–504, Feb. 2009.
- [7] J. D. McKinney, D. E. Leaird, and A. M. Weiner, “Millimeter-wave arbitrary waveform generation with a direct space-to-time pulse shaper,” *Opt. Lett.*, vol. 27, no. 5, pp. 1345–1347, Aug. 2002.
- [8] H. Chi and J. P. Yao, “An approach to photonic generation of high frequency phase-coded RF pulses,” *IEEE Photon. Technol. Lett.*, vol. 19, no. 10, pp. 768–770, May 15, 2007.
- [9] Z. Li, W. Li, H. Chi, X. Zhang, and J. P. Yao, “Photonic generation of phase-coded microwave signal with large frequency tunability,” *IEEE Photon. Technol. Lett.*, vol. 23, no. 11, pp. 712–714, Jun. 1, 2011.
- [10] H. Chi and J. P. Yao, “Photonic generation of phase-coded millimeterwave signal using a polarization modulator,” *IEEE Microw. Wireless Compon. Lett.*, vol. 18, no. 5, pp. 371–373, May 2008.
- [11] Z. Li, M. Li, H. Chi, X. Zhang, and J. P. Yao, “Photonic generation of phase-coded millimeter-wave signal with large frequency tunability using a polarization-maintaining fiber Bragg grating,” *IEEE Microw. Wireless Compon. Lett.*, vol. 21, no. 12, pp. 694–696, Dec. 2011.
- [12] M. Li, Z. Li, and J. P. Yao, “Photonic generation of precisely p phase-shifted binary phase-coded microwave signal,” *IEEE Photon. Technol. Lett.*, vol. 24, no. 22, pp. 2001–2004, Nov. 15, 2012.
- [13] J. D. Bull, N. A. F. Jaeger, H. Kato, M. Fairburn, A. Reid, and P. Ghanipour, “40 GHz electro-optic polarization modulator for fiber optic communications systems,” *Proc. SPIE*, vol. 5577, pp. 133–143, Dec. 2004.
- [14] Q. Wang and J. P. Yao, “A high speed 2×2 electro-optic switch using a polarization modulator,” *Opt. Express*, vol. 15, no. 25, pp. 16500–16505, Dec. 2007.